

# 火山灰追跡モデルPUFFの開発と空中濃度推定

## Development of Volcanic Ash Plume Tracking Model PUFF and Estimation of the Airborne Ash Density

\*田中 博<sup>1</sup>、井口 正人<sup>2</sup>

\*Hiroshi Tanaka<sup>1</sup>, Masato Iguchi<sup>2</sup>

1. 筑波大学計算科学研究センター、2. 京都大学防災研究所

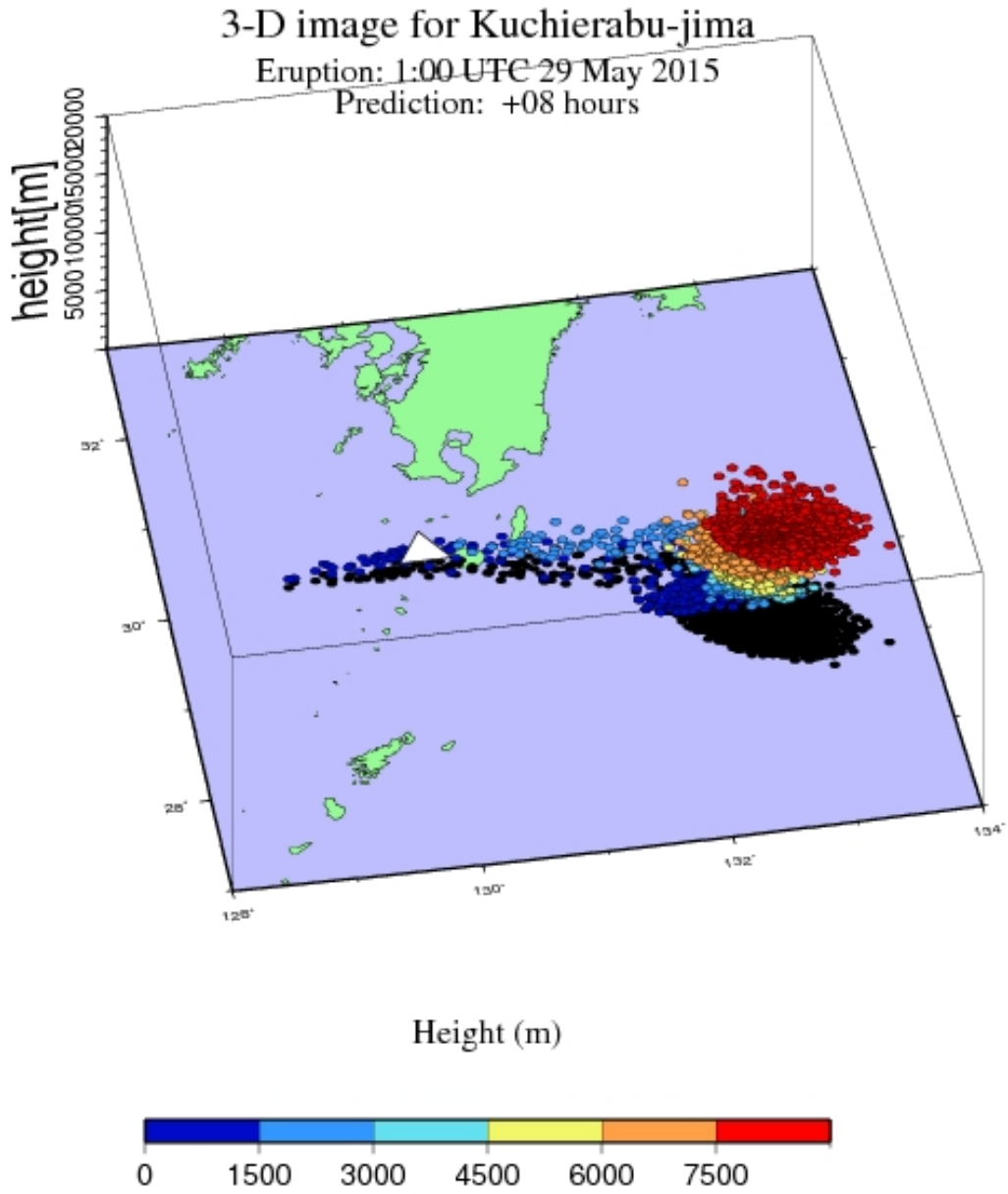
1. Center for Computational Sciences, University of Tsukuba, 2. DPRI, Kyoto University

航空機が空中の火山灰に突入すると、エンジン停止を始めとする航空機の危機的な被害が発生する。したがって、空中を浮遊する高濃度の火山灰は、航空安全上とても危険な存在であり、リアルタイムで空中の濃度分布を推定する必要がある。国際民間航空機関 (ICAO) の情報では、空中に 2 mg/m<sup>3</sup> 以上の濃度の火山灰が存在するとき、その領域は航空機にとって危険とされている。この危険領域をリアルタイムで推定するシステムの構築が望まれている。

本研究では、1990年にアラスカ大学で開発された火山灰追跡モデルPUFFに、世界的に見て観測体制が最も充実している桜島火山を対象に開発されたリアルタイム噴出率推定モデルを結合した火山灰輸送拡散モデルについて説明する。さらに、このモデルを2015年5月に噴出した口永良部島火山に応用し、屋久島での降灰地上観測から空中を浮遊する火山灰の濃度の推定を行った結果を紹介する。空中の火山灰は「ひまわり8号」の衛星画像と同様の輸送拡散を示し、8時間後に火口から200km離れた地点に移動しても100 mg/m<sup>3</sup> の濃度の領域が存在することが推定された。この情報は航空安全にとって重要と考えられる。

キーワード：火山灰予測、火山灰噴出率、航空安全、口永良部島、PUFFモデル、ひまわり8号

Keywords: Volcanic ash plume prediction, Emission rate of volcanic ash, Aviation safety, Kuchinoerabu-jima, PUFF model, Himawari-8



# Fluid dynamics of very large plumes generated by explosive super-eruptions

\*鈴木 雄治郎<sup>1</sup>、コスタ アントニオ<sup>2</sup>、小屋口 剛博<sup>1</sup>  
 \*Yujiro Suzuki<sup>1</sup>, Antonio Costa<sup>2</sup>, Takehiro Koyaguchi<sup>1</sup>

1. 東京大学地震研究所、2. イタリア国立地球物理学火山学研究所

1. Earthquake Research Institute, The University of Tokyo, 2. Institute Nazionale di Geofisica e Vulcanologia

Explosive super-eruptions releasing several hundreds to thousands of km<sup>3</sup> of magma with extremely intense flow rates occurred in the geological past of the Earth. They impacted significantly the climate and global ecosystems. Because of lack of direct observation, plume dynamics of these eruptions are poorly understood. Simple integral models based on the Buoyant Plume Theory (Morton et al., 1956; Woods and Wohletz, 1991) have been commonly used to describe them. The validity of the assumptions behind these models (e.g., self-similarity, constant air entrainment coefficient) should be validated, because the dynamics of super-eruptions can be totally different from a simple buoyant plume. We used a three-dimensional (3D) computational fluid dynamic model (Suzuki et al., 2005) to investigate the main features of these gigantic plumes characterized by Mass Flow Rate (MFR) ranging from 10<sup>9</sup> to 10<sup>11</sup> kg/s. The lower end of the range corresponds to the most intense Plinian columns such as the 1991 Pinatubo eruption, while the upper end to the most extreme co-ignimbrite plumes such as the Toba eruption occurred 74 ka.

We performed 3D simulations of super-eruptions and compared these results with those of the previous models. At the steady-state for low and intermediate MFR, radii of the umbrella cloud spread as function of time with the same asymptotic behavior predicted by simple box models (Woods and Kienle, 1994) and this dependence can be used to estimate MFR. Simulation results also indicate that the co-ignimbrite plume radius, grows with MFR with the same scaling for MFR vs run-out distance predicted by previous simple models of pyroclastic flows by Bursik and Woods (1996). On the other hand, the maximum heights simulated by the 3D model showed the complex dependency on the MFR, which are significantly different from those of the simple integral model (Woods and Wohletz, 1991). This difference indicates that it is necessary to consider new scaling laws of the effective air entrainment coefficients for using the simple integral models as an extrapolation in order to reproduce the gigantic plumes. Results have large implications on the assessment of the intensity and the impact of these explosive super-eruptions on the Earth climate and past ecosystems.

## References

- Bursik, MI, Woods AW (1996) The dynamics and thermodynamics of large ash flows. *Bull Volcanol*, 58:175–193
- Costa, A., et al (2016) Results of the eruptive column model inter-comparison study. *J Volcanol Geotherm Res*, 326: 2–25
- Suzuki, YJ, Koyaguchi, T, Ogawa, M, Hachisu, I (2005) A numerical study of turbulent mixing in eruption clouds using a three-dimensional fluid dynamics model. *J Geophys Res*, 110: B08201
- Woods, A., Kienle, J. (1994), The dynamics and thermodynamics of volcanic clouds: Theory and observations from the April 15 and April 21, 1990 eruptions of Redoubt Volcano, Alaska. *J Volcanol Geotherm Res*, 62: 273–299.
- Woods, AW, Wohletz, K (1991) The dimensions and dynamics of coignimbrite eruption columns. *Nature*, 350:225–227

キーワード：超巨大噴火、火山噴煙、流体力学

Keywords: super-eruption, volcanic plume, fluid dynamics

# Numerical simulations of a two-layer shallow-water model for pyroclastic density current

\*志水 宏行<sup>1</sup>、小屋口 剛博<sup>1</sup>、鈴木 雄治郎<sup>1</sup>

\*Hiroyuki A. Shimizu<sup>1</sup>, Takehiro Koyaguchi<sup>1</sup>, Yujiro J. Suzuki<sup>1</sup>

1. 東京大学地震研究所

1. Earthquake Research Institute, The University of Tokyo

During an explosive volcanic eruption, a hot mixture of volcanic particles and gas is continuously ejected from the volcanic vent and develops an eruption column. When the density of the mixture remains higher than that of the ambient air, the eruption column collapses to produce pyroclastic density currents (PDCs). PDCs are characterized by strong density stratification, whereby a dilute current (particle suspension flow) overrides the dense basal current (fluidized granular flow). The dynamics of PDCs is affected by physical processes within each of the dilute and dense parts, such as thermal expansion of ambient air entrained into the dilute part and basal resistance in the dense part. It also depends on the particle transport between the dilute and dense parts. We aim to understand these effects on PDC dynamics and the resulting run-out distance, by using numerical simulations.

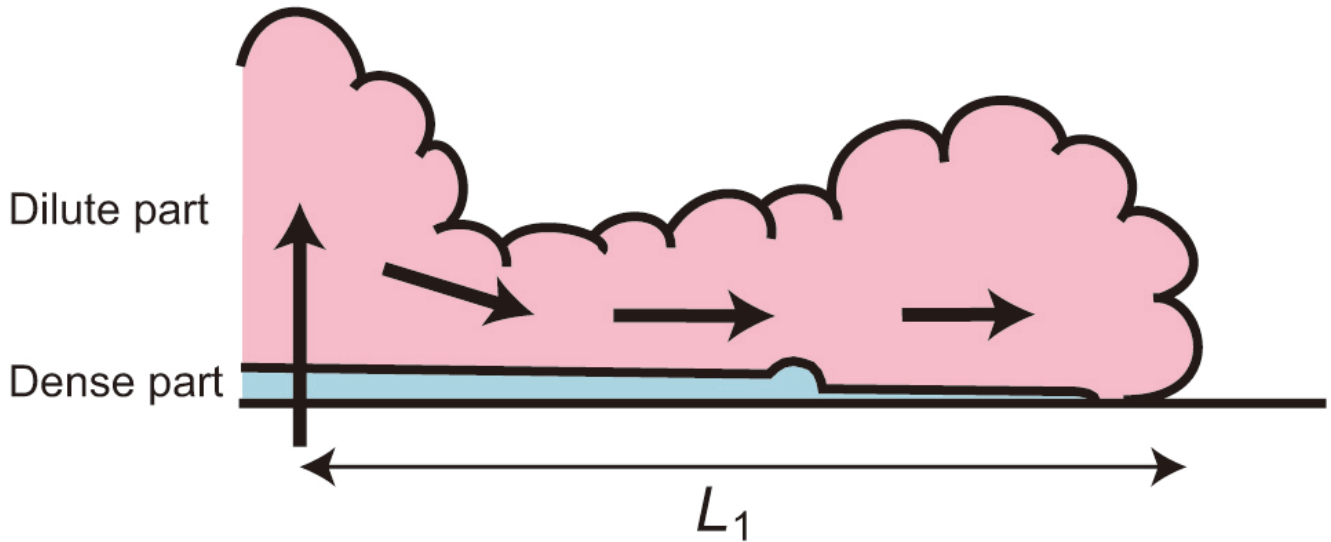
We have developed an unsteady two-layer model to describe density currents with strong density stratification. In this model, each of dilute and dense parts is assumed to be uniform in any vertical section and is formulated by shallow-water equations. In the dilute part, the effects of particle settling, entrainment of ambient air, thermal expansion, interfacial drag between the dilute and dense parts, and resistance of ambient at the flow front are taken into account. In the dense part, the effects of basal resistance, sedimentation, and the particle supply from the dilute part are included. The equations are numerically solved by the finite volume method using the HLL scheme. A stationary dilute mixture with its higher density than that of the ambient air is initially (i.e.,  $t = 0$ ) set in the rectangular reservoir with a solid backwall, and an additional mixture with the same composition as the initial mixture is supplied to the reservoir at a constant rate at  $t > 0$ . A density current is produced on a horizontal ground surface by an instantaneous release of the mixture at  $t = 0$  and the subsequent steady supply of the mixture in the reservoir.

We calculated time evolution of a PDC (e.g., thicknesses and velocities of dilute and dense parts, and thickness of deposit). The result is divided into two stages. In the first stage (Figure 1a), the dilute part propagates, and the dense part develops. Because the dense part propagates slowly owing to basal resistance, the maximum run-out distance in this stage is determined by the front position of the dilute part ( $L_1$ ). In the second stage (Figure 1b), the density of the frontal region of the dilute part falls to that of the ambient air owing to particle settling and thermal expansion of entrained air. The mass of this frontal region ascends from the current into a co-PDC plume (i.e., co-ignimbrite ash cloud), whereas the dilute part around the source forms a steady dilute density current. The run-out distance of the steady current ( $L_s$ ) is much shorter than  $L_1$ . Subsequently, the dense part extends beyond  $L_1$ , and the run-out distance of the PDC is determined by the front position of the dense part ( $L_D$ ).

Previously, the run-out distance of PDC was estimated on the basis of a steady one-layer dilute PDC model (Bursik & Woods, 1996). This run-out distance corresponds to  $L_s$ , and does not represent  $L_1$  or  $L_D$ . Therefore, the run-out distance proposed by the previous study may be underestimated.

キーワード：火砕流、浅水波方程式、2層流モデル、到達距離、粒子サスペンション流、粒子流  
 Keywords: pyroclastic density current, shallow-water equation, two-layer model, run-out distance, particle suspension flow, granular flow

### (a) First stage



### (b) Second stage

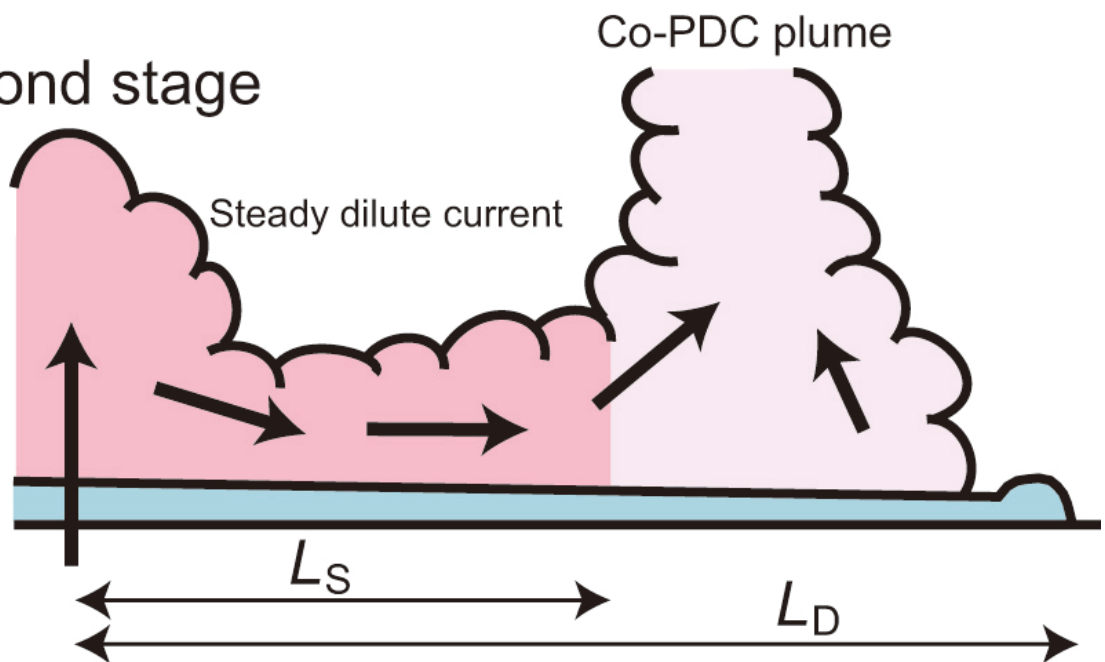


**Figure 1** Schematic illustrations showing time evolution of a PDC.

# A refractive index model of volcanic ash derived from satellite infrared sounder measurements for applications of HIMAWARI-8 retrieval algorithm

\*石元 裕史<sup>1</sup>

\*Hiroshi Ishimoto<sup>1</sup>

1. 気象研究所

1. Meteorological Research Institute

Japan Meteorological Agency (JMA) has been developing a retrieval system to provide volcanic ash products from HIMAWARI-8 infrared measurements through a volcanic ash detection/evaluation algorithm. For the estimation of ash cloud parameters, i.e. cloud top height, optical depth, particle size, and associated mass loading, accurate radiative transfer calculations in the modeled atmosphere are important. Because optical properties of the ash clouds strongly depend on the ash refractive index, a dataset of spectral refractive index in the infrared region for various types of volcanic ash materials is desirable. The current models of refractive index for volcanic ash, which were published more than thirty years ago, are insufficient in spectral resolution as well as in the number of alternatives for the use of multi-channel satellite remote sensing.

As reported in the literatures, refractive index of volcanic rocks and/or ash materials at infrared wavelengths had been estimated in laboratory from the spectral reflectance for the applied infrared light. The situation of satellite infrared sounder measurements for volcanic ash clouds in the atmosphere over land/ocean is essentially similar to the laboratory measurements. It suggests that the ash refractive index can be estimated from the infrared spectroscopy by satellites in condition of no ice/water clouds contamination and if the other unknown parameters, i.e. the ash cloud parameters, the atmospheric profile, and surface temperature/emissivity, are determined in advance or derived simultaneously. The estimated refractive index of the ash material by satellite infrared sounder has a potential to improve volcanic ash retrieval by HIMAWARI-8 for the same ash clouds and also for the ash clouds erupted from the same type of volcanos. In this work, a refractive index model, which derived from the measurements of infrared sounders, AIRS and IASI, for some volcanic events is proposed.

キーワード：火山灰、複素屈折率、ひまわり8号

Keywords: volcanic ash, refractive index, Himawari-8

# 粒径分布の層序変化からみた新燃岳2011年準プリニー式噴火 Temporal variation of the 2011 Shinmoe-dake subplinian eruption inferred from the stratigraphic GSD variation

\*入山 宙<sup>1</sup>、寅丸 敦志<sup>2</sup>

\*Yu Iriyama<sup>1</sup>, Atsushi Toramaru<sup>2</sup>

1. 九州大学大学院理学府地球惑星科学専攻、2. 九州大学 大学院理学研究院 地球惑星科学部門

1. Department of Earth and Planetary Sciences, Graduate School of Science, Kyushu University, 2. Department of Earth and Planetary Sciences, Faculty of Science, Kyushu University

降下火砕堆積物を構成する火砕物の粒径分布は空間的に変化し、噴出物の輸送過程と噴火の時間発展を反映していると考えられる。降下火砕堆積物の粒径分布から噴火現象を復元するために、これまでに我々は噴出物輸送と堆積過程に関する理論的研究を行い、噴火現象と堆積構造の間に成り立つ定量的な関係を導出してきた。本件では降下火砕堆積物の粒径分布の層序変化から噴出初期の粒径分布の時間発展を推定する2次元モデルを新燃岳2011年噴火に応用する。

新燃岳は2011年1月26日から27日にかけて3日の準プリニー式噴火を経験した。一連の噴火現象は、地球物理学的観測によって、噴火最中の噴煙柱高度（新堀・他, 2013）や地殻変動量（Ueda et al., 2013）の時間変化が報告されている。一方、1回目の準プリニー式噴火で形成された降下火砕堆積物中を構成する火砕物の粒径分布は、堆積層下部で上方粗粒化し、その後堆積層上部で上方細粒化している（入山・寅丸, 2015）。2次元モデルを用いて堆積物粒径分布の層序変化を噴出初期の粒径分布の時間変化に変換し、地球物理的に観測された噴火の時間変化と粒径分布の時間変化を直接比較する。

応用の結果推定された噴出初期の粒径分布の時間変化は、粗粒粒子が噴火初期に増加し、噴火後期に減少する変化を示した。粒径分布の時間変化の特徴を定量的に評価するため、推定された粒径分布を時間ごとに冪分布近似を行い、冪数の時間変化を調べた。その結果、噴出初期粒径分布は、噴火初期で冪数が減少（粗粒化）し、噴火後期で冪数が増加（細粒化）することが示された。

定常条件下での噴煙モデル計算により、噴出物の粒径分布、噴出率および最大噴煙高度の関係が得られている（Girault et al., 2014）。本研究によって得られた粒径分布の時間変化および、観測によって得られた噴煙高度の時間変化をモデル計算の結果と比較したところ、噴火中の噴出率の時間変化が示唆された。粒径分布および噴煙高度から期待される噴出率は、噴火初期に噴出率が増加し、噴火後期に噴出率が低下するという時間変化を示し、測地的な観測によって得られる地殻変動量の時間変化と整合的である。

キーワード：粒子サイズ分布、火砕物、時間発展、噴出率

Keywords: grain-size distribution, pyroclasts, temporal variation, mass eruption rate



## Pyrrhotite oxidation as a tool for reconstructing thermal structure of eruption columns

\*松本 恵子<sup>1</sup>、中村 美千彦<sup>2</sup>、鈴木 雄治郎<sup>3</sup>

\*Keiko Matsumoto<sup>1</sup>, Michihiko Nakamura<sup>2</sup>, Yujiro J Suzuki<sup>3</sup>

1. 産業技術総合研究所地質調査総合センター、2. 東北大学理学研究科地学専攻、3. 東京大学地震研究所

1. Geological Survey of Japan, The National Institute of Advanced Industrial Science and Technology, 2. Department of Earth Science, Graduate School of Science, Tohoku University, 3. Earthquake Research Institute, The University of Tokyo

Entrainment of ambient air is a key process in eruption cloud dynamics as it thermally expands and produces buoyancy. Because magma fragments (pyroclasts) are cooled and oxidized by air entrainment, petrological analysis may evaluate independently the entrainment process. To quantify the degree of interaction between fragmented magma and entrained air, we focused on oxidation of pyrrhotite (Po,  $\text{Fe}_{1-x}\text{S}$ ) in the pyroclasts. In this study, we simulated cooling of pyroclasts to examine the coupling between degree of oxidation and eruption dynamics. Cooling of pyroclasts was simulated using a newly-developed routine for a three-dimensional (3-D) eruption column model, while oxidation kinetics of Po are already relatively well understood. By testing the parameter sensitivity of the degree of oxidation and comparing simulated and natural oxidation degrees for a Plinian eruption, we examined the usefulness of Po oxidation as a marker for magma-air interaction and an indicator of eruption-column thermal structure in the 3-D model.

Three simulations with different mass discharge rates and magma temperatures were performed based on the 3-D eruption column model. In the simulations, two types of thermal structures corresponding to jet flow and fountain flow (Suzuki and Koyaguchi 2012) were observed with magma discharge rates of  $10^6$ – $10^7$  kg/s and  $\sim 10^9$  kg/s, respectively. Both of the flow types included an “unmixed core” (or high mass fraction zone) in the column. The fountain-type maintained high temperature longer than the jet-type because the fountain-type unmixed core was not eroded until extensive air entrainment occurred at the top of the fountain.

The oxidation degree of pyroclasts was then calculated on the basis of predicted temperature change of particles in the eruption column. Po in volcanic rocks is often oxidized to form magnetite (Mt,  $\text{Fe}_3\text{O}_4$ ) and then hematite (Hm,  $\text{Fe}_2\text{O}_3$ ) (Matsumoto and Nakamura 2012). The growth rate of Hm from Mt can be applied to measure the oxidation degree of pyroclasts as it has been determined experimentally (Paidassi 1958). Calculations of Hm width were made for approximately 300 to 1000 oxidation markers in the eruption column for each simulation condition, and expressed as frequency distributions of oxidation degree. Our calculations showed that Hm-width distribution varied according to the mass discharge rate (i.e., flow type) and initial magma temperature. The distribution of oxidation degree was broad in the case of fountain-type, whereas it was narrow in the case of jet-type. In addition, an eruption column which has a high initial magma temperature and jet-like structure was characterized by a long-tailed distribution, which results from a presence of high oxidation degree markers. These results indicate that Po oxidation can be potentially used for characterizing the thermal structure of eruption columns.

We also compared calculated Hm widths with petrographic data from the Sakurajima 1914 Plinian eruption. The Hm widths based on the simulation were approximately one-third the thickness of those observed in natural pumices. Three potential explanations for this discrepancy are: (1) thermal conduction of the pumice clasts, which is neglected in the present 3-D model, affects the Po reaction degree; (2) Po reaction rate was underestimated; and/or (3) Po oxidation started in the volcanic conduit before magma fragmentation, possibly accompanying open-system outgassing of the magma.

キーワード：噴煙柱、酸化、磁硫鉄鉱

Keywords: eruption column, oxidation, pyrrhotite

## 火山噴煙の気象レーダー観測

### Volcanic ash plume observation by weather radars

\*佐藤 英一<sup>1</sup>、福井 敬一<sup>1</sup>、新堀 敏基<sup>1</sup>、石井 憲介<sup>1</sup>、徳本 哲男<sup>1</sup>、真木 雅之<sup>2</sup>、井口 正人<sup>3</sup>

\*Eiichi Sato<sup>1</sup>, Keiichi Fukui<sup>1</sup>, Toshiki Shimbori<sup>1</sup>, Kensuke Ishii<sup>1</sup>, Tetsuo Tokumoto<sup>1</sup>, Masayuki Maki<sup>2</sup>, Masato Iguchi<sup>3</sup>

1. 気象研究所、2. 鹿児島大学、3. 京都大学

1. Meteorological Research Institute, 2. Kagoshima University, 3. Kyoto University

これまで、気象レーダーで噴火を観測した事例は数多くある（例えば、澤田（2003）、Marzanoほか（2013））が、定量的な火山灰推定（QAE）技術は未だ確立されていない。その原因のひとつとして、反射強度の不確実性がある。大まかにいえば、このパラメーターは物質の大きさと数の両方を表すが、その2つを分離することが出来ない。言い換えると、反射強度だけでは、粒径分布（PSD）を決定することは出来ない。

そのような状況の中、二重偏波気象レーダーによる火山噴煙の観測が、噴煙内部のPSDに対する情報を得られると期待されている。一般に、二重偏波レーダーは水平と垂直の2つの電波を同時に送信し受信することで、2成分の比や相関係数を得ることが出来る。これらのパラメーターは、QAEに対して有効であると考えられる。

火山噴煙の観測に有効と考えられるもう一つの手段が高速スキャンレーダーである。高速スキャンレーダーによる観測は火山噴煙の3次元画像をわずかな時間で得られるため、この種のレーダーが噴煙のダイナミクスの理解に貢献すると期待している。

気象研究所では、2018年3月からXバンドMPレーダー（MRI-XMP）とKuバンド高速スキャンレーダー（MRI-Ku）による桜島の噴煙観測を開始している。本発表では、桜島の噴火に伴う噴煙のレーダー観測結果を示すとともに、今後の課題や展望について議論する。

#### 参考文献：

澤田可洋, 2003: 気象レーダーで観測された噴煙エコーの記録, 測候時報, **70.4**, 119-169.

Marzano, F. S., E. Picciotti, M. Montopoli, and G. Vulpiani, 2013: Inside volcanic clouds: Remote sensing of ash plumes using microwave weather radars, *Bull. Amer. Meteor. Soc.*, **94**, 1567–1586, DOI: 10.1175/BAMS-D-11-00160.1.

キーワード：火山噴煙、気象レーダー、二重偏波レーダー、高速スキャンレーダー、桜島

Keywords: volcanic ash plume, weather radar, polarimetric radar, fast-scan radar, Sakurajima volcano

# 火山灰拡散予測のための火山灰データ同化システムの開発

## Development of a Volcanic Ash Data Assimilation System for Atmospheric Transport Model

\*石井 憲介<sup>1</sup>、新堀 敏基<sup>1</sup>、佐藤 英一<sup>1</sup>、林 勇太<sup>2,1</sup>、徳本 哲男<sup>1</sup>、福井 敬一<sup>1</sup>、橋本 明弘<sup>1</sup>

\*Kensuke Ishii<sup>1</sup>, Toshiki Shimbori<sup>1</sup>, Eiichi Sato<sup>1</sup>, Yuta Hayashi<sup>2,1</sup>, Tetsuo Tokumoto<sup>1</sup>, Keiichi Fukui<sup>1</sup>, Akihiro Hashimoto<sup>1</sup>

1. 気象研究所火山研究部、2. 気象衛星センター

1. Meteorological Research Institute, 2. Meteorological Satellite Center

In the Japan Meteorological Agency (JMA), there are two major operations related to volcanic ash forecasting: the Volcanic Ash Fall Forecast (VAFF) and the Volcanic Ash Advisory (VAA). The VAFF provides information for local governments and residents who may be affected by ash fall from volcanoes (Hasegawa et al., 2015). The VAA is issued to airline companies and aviation authorities for safe aviation services.

In these operations, the forecasts are calculated by atmospheric transport models including advection process, gravitational fall process and deposition process (wet/dry). The most important and uncertain factor of the models is the initial condition of volcanic ash. In operations, the initial condition is based on the empirical model of Suzuki (1983). Since it includes many assumptions and empirical research, it often fails to reproduce actual plumes of volcanic eruptions.

On the other hand, in recent years, research of observation techniques of volcanic ash by weather radar and satellites have advanced. The Meteorological Research Institute (MRI), one of the facilities of JMA, has started observation using two different types of weather radar. Besides, in 2015, the Himawari-8 geostationary meteorological satellite was put into operation. Himawari-8 has sixteen observation bands as against five in its predecessor, MTSAT-2. Using this abundant observation data of new-generation satellite, physical quantities of volcanic ash clouds (including top height, mass loading and particle radius) can be retrieved (Hayashi et al., JpGU2016).

In the present study, using both radar and satellite observation, we are developing a volcanic ash data assimilation system to improve initial conditions of the atmospheric transport models.

We have adopted the three-dimensional variational data assimilation scheme (3D-Var), which has low computational cost and is suitable for creating initial conditions immediately after an eruption occurs. Analysis variables are concentration of ash and size distribution parameters (median particle size and dispersion) which are mutually independent. It is assumed that observation error covariance matrix is diagonal, and background error covariance matrix has the relationship between correlation and distance and has the Gaussian form (Ishii et al., JpGU2016).

From the radar observation, it is expected that we can obtain three-dimensional ash concentration in the atmosphere and parameters of ash particle size distribution in the atmosphere. On the other hand, the satellite observation is expected to provide only two-dimensional parameters of ash clouds such as mass loading, top height and particle radius. Currently, we are trying to estimate the thickness of ash clouds using vertical wind shear.

Here, we show two case studies of data assimilation system. One is the February 14th, 2014 eruption case of Kelut in Indonesia for an experiment of data assimilation with virtual radar observation, and the other is the May 29th, 2015 eruption case of Kuchinoerabujima in Japan for an experiment of data assimilation with actual satellite observations.

References

- Hasegawa, Y., A. Sugai, Yo. Hayashi, Yu. Hayashi, S. Saito and T. Shimbori, 2015: Improvements of volcanic ash fall forecasts issued by the Japan Meteorological Agency. *J. Appl. Volcanol.*, **4**: 2.
- Hayashi, Y., D. Uesawa, K. Bessho (2016) Observation of volcanic ash clouds by Himawari-8. JpGU 2016, MIS26-06.
- Ishii, K., T. Shimbori, K. Fukui, E. Sato, A. Hashimoto (2016) Real-time data assimilation of radar-based volcanic ash data in an atmospheric transport model. JpGU 2016, MIS26-P04.
- Suzuki, T., 1983: A theoretical model for dispersion of tephra.:Arc volcanism: Physics and tectonics, D. Shimozuru and I. Yokoyama, editors, *TERRAPUB, Tokyo*, 95-113.

キーワード : データ同化、移流拡散モデル、火山灰

Keywords: data assimilation, atmospheric transport model, volcanic ash

## ひまわり8号30秒データで見た噴火直後の火山噴煙

### Observations of volcanic eruption columns using Himawari-8 Super-Rapid Scan 30-sec imagery

\*福井 敬一<sup>1</sup>、佐藤 英一<sup>1</sup>、林 勇太<sup>2,1</sup>、松田 康平<sup>3</sup>、石井 憲介<sup>1</sup>、新堀 敏基<sup>1</sup>、徳本 哲男<sup>1</sup>

\*Keiichi Fukui<sup>1</sup>, Eiichi Sato<sup>1</sup>, Yuta Hayashi<sup>2,1</sup>, Kohei Matsuda<sup>3</sup>, Kensuke Ishii<sup>1</sup>, Toshiki Shimbori<sup>1</sup>, Tetsuo Tokumoto<sup>1</sup>

1. 気象研究所火山研究部、2. 気象衛星センター、3. 気象庁火山課

1. Meteorological Research Institute/JMA, 2. Meteorological Satellite Center/JMA, 3. Japan Meteorological Agency

気象庁は2015年7月7日より、次世代静止気象衛星ひまわり8号の運用を開始した。ひまわり8号に搭載された可視赤外放射計 (Advanced Himawari Imager, AHI) は、前代のひまわり7号MTSAT-2に搭載されていた放射計に対し、観測波長帯数が5バンド (可視1, 赤外4) から16バンド (可視3, 近赤外3, 赤外10) へと大幅に増強され、空間分解能もほぼ倍に高解像度化した。さらに、全球の観測頻度も60分ごとから10分ごとに向上するとともに、日本域 (東西2000 km, 南北1000 kmに2分割) や台風観測などに利用される東西南北1000km四方の可動領域では常時2.5分ごとの観測も可能となっている (領域観測1, 2, 3)。また、東西1000km, 南北500kmの領域2か所 (領域観測4, 5) を常時約30秒ごとに観測している。この観測は、主に位置合わせや月を利用した感度校正を目的としている (Bessho *et al.* 2016) が、火山噴火や積乱雲の観測にも活用可能であり、最近では試験的に、桜島や浅間山などを含む領域を対象として観測していることも多い。

ひまわり8号の高解像度・高頻度観測によってMTSATに比べ小さな噴火も観測可能となるとともに、多バンド化によって、火山灰雲高度推定の精度向上と、火山灰雲の光学的厚さや粒径などの情報を含む火山灰プロダクトの開発が進められている (Hayashi *et al.* 2016)。さらに、火山ガス (SO<sub>2</sub>) の検出も可能となってきている。

我々は、噴火直前の火口の温度状況や噴火直後の噴煙柱の成長の様子を捉えるため、30秒ごとの超高頻度観測 (Super-Rapid Scan) データを利用した研究を開始した。手始めに、空間分解能0.5kmのバンド3 (0.64 μm) による桜島爆発時の噴煙柱のひまわり画像と監視カメラ、気象レーダーデータ (Sato *et al.* 2017) を比較し、ひまわり画像によって噴煙柱の上昇過程をどの程度把握可能か調査した。

#### 参考文献

Bessho, K. *et al.* (2016) An Introduction to Himawari-8/9 —Japan's New-Generation Geostationary Meteorological Satellites. *J. Meteor. Soc. Japan*, **94**, 151-183, DOI:10.2151/jmsj.2016-009.

Hayashi, Y. *et al.* (2016) Observation of volcanic ash clouds by Himawari-8. JpGU 2016, MIS26-06.

Sato, E. *et al.* (2017) Volcanic ash plume observation by weather radars. JpGU2017.

キーワード：ひまわり8号、30秒データ、噴煙柱、火山噴火、静止気象衛星、桜島

Keywords: Himawari-8, Super-Rapid Scan, eruption column, volcanic eruption, geostationary meteorological satellite, Sakurajima volcano

## A sequence of plinian eruption preceded by dome destruction at Kelud volcano, Indonesia, on February 13, 2014: insights from tephra fallout and pyroclastic density current deposits

\*前野 深<sup>1</sup>、中田 節也<sup>1</sup>、吉本 充宏<sup>2</sup>、嶋野 岳人<sup>3</sup>、外西 奈津美<sup>1</sup>、Zaennudin Akhmad<sup>4</sup>、井口 正人<sup>5</sup>  
\*Fukashi Maeno<sup>1</sup>, Setsuya Nakada<sup>1</sup>, Mitsuhiro Yoshimoto<sup>2</sup>, Taketo Shimano<sup>3</sup>, Natsumi Hokanishi<sup>1</sup>, Akhmad Zaennudin<sup>4</sup>, Masato Iguchi<sup>5</sup>

1. 東京大学地震研究所、2. 山梨県富士山科学研究所、3. 常葉大学大学院環境防災研究科、4. Centre for Volcanology and Geological Hazard Mitigation, Bandung, Indonesia、5. 京都大学防災研究所火山活動研究センター

1. Earthquake Research Institute, University of Tokyo, 2. Mount Fuji Research Institute, Yamanashi Prefectural Government, 3. Graduate School of Environmental and Disaster Research, Tokoha University, 4. Centre for Volcanology and Geological Hazard Mitigation, Bandung, Indonesia, 5. Disaster Prevention Research Institute, Kyoto University

A plinian-style eruption with a radially spreading umbrella cloud occurred on February 13, 2014, at Kelud volcano, Indonesia. We present the sequence of this plinian event based on a geological study of the eruptive products, analysis of satellite images of the eruption plume, and surface features of the volcanic edifice before and after the eruption. The eruptive deposits were divided into four major depositional units (Units A, B, C, and D) and used to determine the sequence of events. The plinian phase was preceded by partial destruction of the existing lava dome and generation of high-energy pyroclastic density currents (PDCs) with a maximum runout distance of ~6.8 km mainly towards the NE. The PDCs produced a series of depositional subunits (Units A<sub>0-2</sub>) and caused surface damage (blown-down trees and vegetation) over an area of 12 km<sup>2</sup> (stage 1). The main phase of the eruption was characterized by a strong eruption plume that produced widespread fallout tephra (Unit B) over East and Central Java (stage 2). The winds above the volcano significantly affected the tephra dispersal process. In stage 3, the plinian column collapsed, generating dense PDCs that flowed down the volcano valleys, producing pumiceous lobate deposits (Unit C). The declining phase of the eruption produced fine-rich fallout tephra layers (Unit D<sub>1-2</sub>) from low-level eruption plumes and/or ash lofted from PDCs. The eruption sequence constructed from field observations is supported by geophysical observations, including remote seismic and infrasound signals, total electron content variation, lightning strokes, and satellite observations. The initial high-energy PDCs and fallout tephra contained juvenile pumice and dome-derived lithic clasts, and isolated crystals originated from the fragmentation of porphyritic magma. The deposit features and componentry suggest that newly ascended magma triggered the destruction of the lava dome and the generation of high-energy PDCs, and during the subsequent climactic phase the dome was completely destroyed. Thus, the pre-existing lava dome significantly affected the course of the eruption. This type of eruption sequence has not been previously documented in the historical records of Kelud volcano activity. The total volume of erupted material was estimated as 0.25–0.50 km<sup>3</sup> (bulk deposit volume), corresponding to 0.14–0.28 km<sup>3</sup> in DRE, and the mean eruption rate as  $6.5 \pm 2.8 \times 10^7$  kg/s. The scale of the 2014 eruption had a VEI of 4, and was one of the largest eruptions at Kelud volcano over the past century. The eruption sequence and estimated physical parameters of the 2014 eruption will help assess future volcanic activity and potential hazards at Kelud volcano.

キーワード：プリニアン、火砕物密度流、倒木、溶岩ドーム、ケルウト

Keywords: Plinian, pyroclastic density current, blown-down tree, lava dome, Kelud

# 浮力増加を伴う乱流プルームの一次元定常モデルの構築と火山噴煙への適用

## A One-dimensional Steady State Model of a Buoyancy-generating Turbulent Plume and its Application to Volcanic Eruption Columns

\*石峯 康浩<sup>1</sup>

\*Yasuhiro Ishimine<sup>1</sup>

1. 国立保健医療科学院健康危機管理研究部

1. Department of Health Crisis Management, National Institute of Public Health

高さとともに浮力フラックスが増加する乱流プルームの一次元定常モデルについて発表する。噴煙柱の基本的な特徴を適切に表現するには、火山噴煙に取り込まれる大気の熱膨張によって浮力フラックスが増加することを定式化することが重要であると考えからである。初めに、一様な静止流体中で浮力フラックスが高さに比例して増加する仮想的な軸対象の乱流プルームに関して議論し、プルーム内の流体の上昇速度が高さによらず一定という解析解が得られることを示す。この結果は、上昇速度が高さの1/3乗に比例して減少するという非圧縮乱流プルームの解と対照的である。一様な流体ならびに成層流体中のより現実的な乱流プルームに関しても上のモデルを修正して議論し、いくつかの特徴的な長さスケールを導入する。これらの長さスケールを使って浮力が増加する場合の乱流プルームの到達高度についても議論する。これらの長さスケールを使った数値解析により、実際の火山噴煙では最高高度に到達する前に熱エネルギーを大気を膨張させるためにすべて消費してしまっていることが示唆された。また、実際の火山噴煙柱内の浮力フラックスは、従来の非圧縮流体の乱流プルームに関する理論で見積もられているものの半分以下である可能性も示唆された。今回、構築した一次元モデルは、噴煙柱の“超浮力的な振る舞い”に関する物理背景についても新たな知見をもたらしたと考えられるので、この点についても発表する。

キーワード：噴煙柱、乱流プルーム、一次元モデル、浮力フラックス、熱膨張

Keywords: Eruption column, Turbulent plume, One-dimensional model, Buoyancy flux, Thermal expansion



# 桜島火山近傍LIDAR観測による火山噴出物の散乱特性

## Backscattering characteristic of volcanic eruptions based on LIDAR observation around Sakurajima Volcano

\*日向 洋<sup>1</sup>、井口 正人<sup>2</sup>、鍵山 恒臣<sup>1</sup>

\*Hiroshi Hinata<sup>1</sup>, Masato Iguchi<sup>2</sup>, Tsuneomi Kagiya<sup>1</sup>

1. 京都大学大学院理学研究科、2. 京都大学防災研究所附属火山活動研究センター

1. Graduate school of Science, Kyoto University, 2. Sakurajima Volcano Reserach Center, Disaster Prevention Reserach Institute, Kyoto University

火山から遠方に設置されたLIDAR (Light detection and Ranging) によって噴火後に大気中を浮遊している火山灰が観測され、粒子によるレーザー光の散乱を示す散乱強度や粒子の非球形度を示す偏光解消度について議論されてきた (例えば, Sassen et al., 2007). 本研究では, 2009年以降, 火山噴火が多発する桜島火山の昭和火口の上空を対象としてLIDAR観測を行い, 火山灰を含む噴煙および白色噴煙の散乱強度と偏光解消度の時間変化および空間分布を明らかにした.

白色噴煙は偏光解消度の最頻値が火口上空において0.05~0.10と雲と同様の値となったことから, 水滴からなることが確かめられた. 散乱強度は火口周辺で最大値となり, 移流される方向に離れていくにしたがって, 低下するが, 偏光解消度は増加した. 水滴の蒸発速度を求め, 乾燥した大気との接触により火口上空では多かった水滴が蒸発し, 非球形粒子の火山灰粒子の割合が相対的に高くなっていったと推定した.

一方, 爆発時に放出された火山灰を含む噴煙の偏光解消度は最頻値が0.40~0.45と, 雲および白色噴煙と比較して大きくなった. 特に, 爆発噴火発生直後の火口上空では最大0.72の偏光解消度が得られた. この高い偏光解消度は火口から離れると, 急激に低下し, 0.45~0.50の値に収束した. 火口上空は非球形粒子である火山灰濃度が高く, 高い偏光解消度が得られたものと考えられる. 一方, その低下については, 火山灰粒子の拡散および落下による火山灰粒子の濃度の減少や, 噴煙上昇に伴う上昇気流または噴煙の冷却により生成された水滴の混入がその原因と推測できる.

キーワード : 白色噴煙、火山灰を含む噴煙、ライダー、散乱強度、偏光解消度、桜島火山

Keywords: Volcanic smoke colored white, Volcanic smoke include volcanic ash, LIDAR, Backscattering intensity, Depolarization ratio, Sakurajima Volcano